

Increased sediment transport via bioturbation at the last glacial-interglacial transition

Matthew W. Hughes¹, Peter C. Almond¹, and Joshua J. Roering^{2*}

¹Soil and Physical Sciences Group, P.O. Box 84, Lincoln University, Lincoln 7647, Canterbury, New Zealand

²Department of Geological Sciences, University of Oregon, Eugene, Oregon 97403-1272, USA

ABSTRACT

Global sedimentation rates increased during the Quaternary due to frequent landscape adjustment to climatic oscillations. Although high rates of sediment transport are commonly associated with glacial conditions in mountainous terrain, the influence of climate and vegetation on geomorphic response is poorly constrained outside of glaciated settings. Along a low-gradient (<30%) hillslope-valley transect on a moderately dissected, loess-mantled fluvial terrace in the Charwell Basin, New Zealand, we coupled records of colluvial infilling and vegetation change (via phytoliths) to show that late Pleistocene sediment flux was $\sim 0.0012 \text{ m}^3 \text{ m}^{-1} \text{ a}^{-1}$ under a shrubland/grassland mosaic and Holocene sediment flux was $\sim 0.0022 \text{ m}^3 \text{ m}^{-1} \text{ a}^{-1}$ under forest. This near doubling through the last glacial-interglacial transition appears to reflect increased bioturbation and downslope soil transport associated with a forest ecosystem. Such an increase in sediment transport contrasts with a contemporaneous decrease inferred for adjacent steep, landslide-prone catchments, suggesting that geomorphic response to climate change is heavily modulated by biology, topography, and geological substrate. Our findings appear to contradict the commonly cited notion that forest colonization universally stabilizes soils and suppresses erosion. Instead, over long time scales, bioturbation associated with forests may increase transport along gentle portions of the landscape not subject to slope instability or erosion by overland flow.

INTRODUCTION

The onset of Quaternary climate variability corresponds with a global increase in terrestrial sediment flux to proximal basins (e.g., Molnar, 2004) and accelerated orogenic exhumation (e.g., Shuster et al., 2005). This increase has been attributed to persistent erosion as landscapes, which have response times greater than the period of climate change, perpetually adjust between equilibrium forms (Zhang et al., 2001). These climate-driven variations appear to vary strongly with tectonic setting and regional climate characteristics. In the semi-arid to arid Colorado Plateau, for example, monsoonal precipitation patterns returned with the end of glacial conditions and induced higher erosion rates during the Holocene (e.g., McFadden and McAuliffe, 1997). By contrast, in the subhumid Seaward Kaikoura Range, New Zealand, Bull (1991) used terrace records to postulate that accelerated sediment flux occurred during glacial periods due to sparse vegetation, pervasive soil stripping, and shallow landsliding. This geomorphic response model has been broadly applied to mountainous landscapes across the globe and is often invoked to explain regional-scale fluvial patterns, such as cyclic terrace formation. Unfortunately, records of terrace formation and basin sedimentation reflect catchment-averaged landscape dynamics and thus are substantially disconnected from process-scale geomorphic responses to climate

change. At the hillslope scale, for example, we have a poor understanding of how vegetation change modulates the rate of sediment delivery to channel networks.

On hillslopes, the geomorphic role of vegetation is multifold; plant and root systems influence the hydrologic cycle, hydrologic properties, soil shear strength, and the vigor of soil disturbance. Numerical models are beginning to incorporate these effects in coupled simulations of landscape evolution (e.g., Istanbulluoglu and Bras, 2005), but sparse quantitative field data exist for model testing and calibration. At our New Zealand study site, we quantify biogenic controls on sediment transport through the last glacial-interglacial transition by reconstructing the infilling of an unchanneled valley and documenting associated changes in vegetation. We use diverse tools, including primary and colluvial loess records, a well-documented late Quaternary tephra, and plant phytoliths to characterize geomorphic and ecological interactions along an $\sim 100 \text{ m}$ slope-valley transect. Our findings challenge the notion that forest colonization universally decreases rates of sediment transport.

STUDY SITE: CHARWELL BASIN, SOUTH ISLAND, NEW ZEALAND

Charwell Basin is a 6-km-wide structural depression to the immediate south of the Seaward Kaikoura Range in northeastern South Island, New Zealand (Fig. 1A). The Seaward Kaikoura Range is composed of Cretaceous

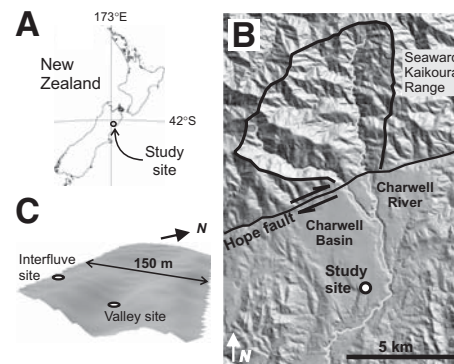


Figure 1. A: Location of the Charwell Basin in South Island, New Zealand. B: Shaded relief map of Charwell Basin and Seaward Kaikoura Range, with location of the study site indicated. C: Local perspective shaded relief map of interfluvial and valley sampling sites.

folded and faulted, massive to medium-bedded graywackes and argillites of the Pahau terrane. The mountainous catchment of the Charwell River and the adjacent range front basin are separated by the Hope fault, a 220-km-long, active splay of the South Island Marlborough fault zone. High rates of right-lateral slip (20 mm a^{-1} ; Wallace et al., 2007) and range-side uplift ($1\text{--}3 \text{ mm a}^{-1}$) along the fault allow for the accumulation, translocation, and preservation of alluvial deposits within the basin (Fig. 1B). Terrace remnants are progressively older and more dissected southwest of the current Charwell River location (Bull, 1991). The number of loess sheets (and buried soils) on the alluvial terraces increases systematically with terrace age (Tonkin and Almond, 1998). A pollen-based reconstruction of late Pleistocene paleovegetation places Charwell Basin within a zone of “dry open grassland with some shrubs” (Alloway et al., 2007). During the Holocene, mean annual temperature and mean annual rainfall equal to 10°C and 1200 mm , respectively, supported beech and podocarp forests before widespread European land clearing.

Bull (1991) proposed that during glacial periods, frost processes and sparse vegetation in the steep, bedrock-dominated Seaward Kaikoura Range led to pervasive soil stripping and landsliding. In combination with the reduced stream power of the Charwell River, the increase in sediment production caused aggradation in

*E-mail: jroering@uoregon.edu

Charwell Basin. During interglacial periods, dense vegetation became re-established in the upland catchment, and terraces were formed in the basin as the sediment-starved Charwell River incised (Fig. 1B).

Our low-gradient (<30%), hillslope–unchanneled valley transect in Charwell Basin is located on a >150 ka old fluvial terrace remnant mantled by three loess sheets that total ~5 m in thickness (Roering et al., 2004). Given its position near the headwaters of a small (<0.5 km²) tributary, our site is isolated from erosion and deposition associated with the mountainous Charwell catchment on the opposite (upthrown) side of the Hope fault (Fig. 1B). In addition, our transect is situated >200 m upstream of the active channel head and a zone of steep channel gradients, indicating that it has been insulated from cut and fill cycles since initial gullying of the terrace gravels ended and loess infilling began. Erosion by overland flow is absent despite the historical conversion of forest to pasture, and the gentle slope gradients at our site (<30%) preclude slope failure. Thus, our results primarily reveal temporal variations of disturbance-driven transport processes (i.e., soil creep) from side slopes into the unchanneled valley (Fig. 1C).

METHODS

To determine mass flux rates associated with forested Holocene and grassland/shrubland late Pleistocene valley deposits, we determined the dimensions and densities of Holocene and late Pleistocene valley deposits as well as the depth of chronostratigraphic markers. This approach is similar in principle to that employed by Reneau et al. (1986) for colluvial hollows. We collected numerous vertically oriented, continuous auger samples from the interfluvium and valley. Using a backhoe, we dug >2.5 m deep trenches at several locations along the transect, allowing us to document near-surface soil stratigraphy with high precision. Microscopic concentrations of volcanic glass identified as Kawakawa/Oruanui tephra by electron microprobe analyses established a $27,097 \pm 957$ cal. yr B.P. (mean \pm standard deviation) datum (Lowe et al., 2008) at 0.8 m and 2.6 m depths at the interfluvium and valley axis, respectively (Fig. 2). We also collected depth profiles of the fallout nuclide ¹³⁷Cs on the interfluvium and valley fill to determine whether historical land-use practices have substantially contributed to valley infilling.

We distinguished sediment accumulated under Pleistocene shrubland/grassland from that accumulated under Holocene forest by analyzing phytolith assemblages. The timing of this transition is given by the calibrated radiocarbon age of $10,690 \pm 1690$ cal. yr B.P. (McGlone and Basher, 1995) on local subfossil tree material. To remove the eolian component of the valley deposit that accumulated during the late Pleis-

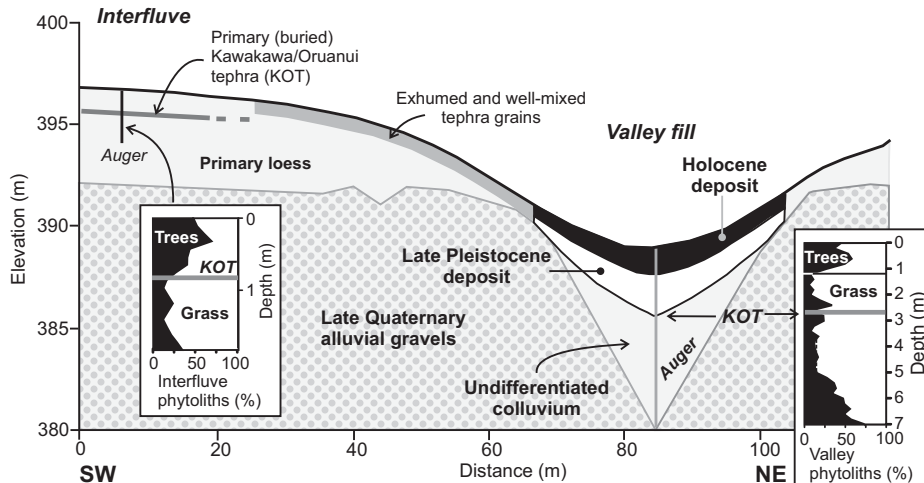


Figure 2. Diagrammatic representation of the hillslope–unchanneled valley transect. Stratigraphy is based on auger and trench observations.

tocene, and thereby isolate the component contributed by slope processes, we estimated the thickness of loess above the Kawakawa/Oruanui tephra from the flat, uneroded interfluvium at the top of the catena as 0.8 ± 0.1 m (Fig. 2). By assuming spatially uniform loess flux, we are likely to underestimate the eolian component in the valley fill (Goossens, 1988) and thereby overestimate the flux of slope-derived sediment in the late Pleistocene. Consistent with Pillans (1994) we assume loess stopped accumulating at the Pleistocene–Holocene transition such that the loess component in the Holocene valley fill is negligible. To enable calibration of a sediment transport model for Holocene (forest) and late Pleistocene (grassland/shrubland) conditions, we performed high-precision topographic surveys of the two opposing slopes that contribute soil to the valley.

CLIMATE-DRIVEN VEGETATION CHANGE AND SEDIMENT FLUX

The valley and interfluvium phytolith distribution profiles show general agreement, except that the valley fill record is substantially “stretched” reflecting the input of material from the adjacent slopes (Fig. 2). In the valley fill, the abundance of tree phytoliths increased from a minimum of 5% during the Last Glacial Maximum to a maximum of 55% in the Holocene (Fig. 2). In the compressed interfluvium record, tree phytolith abundance was slightly higher at the time of the Kawakawa/Oruanui tephra than in the valley. Tree phytoliths on the interfluvium may be overrepresented due to downward translocation via bioturbation, whereas ongoing deposition in the valley may have resulted in a record more representative of local paleovegetation. Small-scale variations in phytolith abundance may also reflect forest density driven by soil and hydrologic factors.

Most importantly, tree phytolith abundances >60% in the top 40 cm of the interfluvium and in the top 1.0 m of the valley fill are indicative of a local Holocene tall beech/podocarp forest in the region (Wardle, 1991).

To calculate late Pleistocene (grassland) and Holocene (forest) soil flux rates, we estimated mass accumulation per unit cross section for the northwest half of the roughly symmetrical valley deposit. The late Pleistocene mass flux, q_{LP} (kg m⁻¹ a⁻¹), is calculated by subtracting the loess component from the total mass of the late Pleistocene deposit according to

$$q_{LP-mass} = \frac{(\rho_{LP}h_{LP} - \rho_L h_L)w_{LP}}{t_{LP}}, \quad (1)$$

where ρ_{LP} and ρ_L are the bulk densities of late Pleistocene valley deposits and loess (kg m⁻³), respectively; h_{LP} and h_L are the thicknesses of late Pleistocene and loess deposits (m), respectively; w_{LP} is the average half width (m) of the late Pleistocene valley fill; and t_{LP} is the late Pleistocene time period (a). The Holocene mass flux (kg m⁻¹ a⁻¹) into the valley is calculated as

$$q_{H-mass} = \frac{\rho_H h_H w_H}{t_H}, \quad (2)$$

where ρ_H is the bulk density of the Holocene valley fill (kg m⁻³), h_H is the Holocene deposit thickness (m), w_H is the Holocene deposit half width (m), and t_H is the Holocene time period (a), which was not subject to loess deposition. Volumetric soil fluxes for the late Pleistocene (q_{LP}) and Holocene (q_H) can be calculated by dividing equations 1 and 2, respectively, by the average soil bulk density, ρ_s (kg m⁻³), measured along the hillslope transect.

Phytolith profiles obtained in the valley fill show a clear shift from grassland to forest at just greater than 1 m depth. The extent of these forest-dominated sediments across the valley floor demarcates Holocene infilling of our unchanneled valley according to the nearby chronology of McGlone and Basher (1995) (Fig. 2). Sediments underlying the Kawakawa/Oruanui tephra represent late Pleistocene material accumulated under grassland/shrubland. Differences in the ^{137}Cs activity profiles on the interfluvium and in the valley axis are negligible (Fig. DR1 in the GSA Data Repository¹), confirming that recent land-use practices have not perceptibly contributed to valley infilling. In addition, soil stratigraphic observations from our trench and auger sites in the valley fill did not reveal buried soils, unconformities, or other evidence for episodic incision and aggradation. As a result, temporal variability in the accumulation of valley fill deposits reflects long-term climate and vegetation controls on sediment transport. From our reconstruction of the valley deposit geometry and chronology, the Holocene forest transport rate, q_{H^*} of $0.0022 \pm 0.0007 \text{ m}^3 \text{ m}^{-1} \text{ a}^{-1}$ is nearly twice that of the late Pleistocene grassland/shrubland transport rate, q_{LP^*} of $0.0012 \pm 0.0005 \text{ m}^3 \text{ m}^{-1} \text{ a}^{-1}$ (Table 1).

In the absence of overland flow, numerous studies have modeled soil transport as a slope-dependent process and estimated flux rates as proportional to slope angle in areas of relatively gentle relief (Kirkby, 1971). The proportionality constant between soil flux and hillslope gradient encapsulates how the frequency, magnitude, and depth of disturbances in the soil mantle contribute to sediment transport. We approximate soil transport rate constants, K ($\text{m}^2 \text{ a}^{-1}$), individually for the late Pleistocene (shrubland/grassland) and Holocene (forest) time periods as $K = q_v/(dz/dx)$, where q_v is the volumetric sediment flux rate ($\text{m}^3 \text{ m}^{-1} \text{ a}^{-1}$), and dz/dx is the gradient near the base of

the southeast-facing slope (Table 1). Given the topographic gradient for the southeast-facing slope that contributes to the valley fill (25% or 0.25), associated K values for the Holocene and late Pleistocene are $0.0088 \pm 0.003 \text{ m}^2 \text{ a}^{-1}$ and $0.0047 \pm 0.002 \text{ m}^2 \text{ a}^{-1}$, respectively.

DISCUSSION AND CONCLUSIONS

The combined valley infilling and phytolith records presented here demonstrate that Holocene establishment of beech and podocarp forest in Charwell Basin significantly increased soil transport rates. This finding highlights the importance of biogenic processes in shaping Earth's surface (Dietrich and Perron, 2006), particularly given the variability of climate through the Quaternary. At first glance, our results appear to contradict the well-established notion that reforestation stabilizes soil and suppresses erosion by shallow landsliding and overland flow. With respect to overland flow, the addition of any vegetation to a bare soil surface will tend to increase infiltration rates as well as the hydraulic threshold for incision and entrainment. Given the absence of overland flow erosion at our study site (even during current humid and pasture conditions) and at nearby sites under dense native forest, we infer that our results do not reflect changes associated with overland flow. With respect to shallow landsliding, the soils of our site exhibit high shear strength, and the slopes never achieve inclinations greater than 30% (or 16°) and do not exhibit evidence of slope instability.

Instead, we suggest that the dominant geomorphic impact of a grassland-to-forest transition at our site is an increase in the rate and style of bioturbation. Over short time scales, tree root networks effectively bind and stabilize soils, but over 100- to 1000-year time scales, tree turnover and related disturbances ensue, resulting in significant downslope translation of material (Gabet et al., 2003). On the interfluvium of our

study site, previous analyses of Kawakawa/Oruanui tephra distributions attest to the increased vigor of bioturbation with forest colonization (Roering et al., 2002). The Kawakawa/Oruanui tephra was emplaced ca. 27 ka ago during a period of slow but steady loess accumulation. The grass-dominated vegetation mosaic during this period induced relatively minor mixing (or bioturbation) of tephra grains as upbuilding of the soil column continued, resulting in a narrow, readily defined tephra concentration peak at ~ 0.8 m depth. At downslope locations, where erosion has subsequently exhumed the concentration peak into the rooting zone of beech and podocarp trees, the peak is absent and concentrations are uniformly low ($\sim 15\%$ of the peak value) in the upper 40–50 cm of soil (Roering et al., 2002). This pattern suggests vigorous soil mixing during Holocene forest conditions. When coupled with the results presented in this paper, these mixing data suggest that bioturbation rate may be a first-order control on downslope sediment flux in low-gradient, soil-mantled landscapes (Kaste et al., 2007).

We interpret these findings as evidence for a mobile bioturbation formed by floralturbation (Johnson, 1990). Specific mechanisms by which soil is moved downslope likely include tree uprooting, post-turnover soil redistribution via rainsplash, microburrowing, soil dilation and transport via root growth, and gravitational collapse as root plates decompose (Gabet et al., 2003). Unfortunately, our results cannot distinguish the relative importance of such individual mechanisms. Other studies have concluded that floral turbation is a major process influencing soil profiles and local topography in forested landscapes (e.g., Denny and Goodlett, 1956; Schaetzl et al., 1990) by estimating root plate volumes and disruption of soil horizons. According to Norton (1989), rates of tree turnover are sufficient to stir more than 50% of forest floor area on 100- to 1000-year time scales.

The empirically derived Holocene K value of $0.0088 \text{ m}^2 \text{ a}^{-1}$ calculated here is similar to those estimated by Denny and Goodlett (1956; $\sim 0.010 \text{ m}^2 \text{ a}^{-1}$) in a forested landscape. As revealed from paleosurface profiles at our study site (Roering et al., 2004), the transition from rectilinear hillslope segments under late Pleistocene grassland/shrubland mosaic to a convex form with forest colonization in the Holocene also supports our conclusion of increased sediment transport. In fact, such a change in hillslope form also suggests that the difference in our Holocene and late Pleistocene K values (which reflect sediment transport efficiency) may be underestimated given that transport likely decreased through the Holocene via progressive slope decline.

TABLE 1. CALCULATION OF HOLOCENE AND LATE PLEISTOCENE SOIL FLUX RATES (MEAN \pm STANDARD DEVIATION)

Variable	Holocene	Late Pleistocene (post-KOT*)
t , time (a)	10,690 \pm 1690	16,407 \pm 2647
h , deposit thickness (m)	1.2 \pm 0.1	1.6 \pm 0.1
w , mean deposit half width (m)	16 \pm 1	14 \pm 1
h_L , post-KOT* loess thickness (m)	—	0.8 \pm 0.1
ρ_S , soil bulk density (kg m^{-3})	1350 \pm 140	1350 \pm 140
ρ_L , loess bulk density on interfluvium (kg m^{-3})	—	1471 \pm 150
ρ_{H^*} , Holocene deposit bulk density (kg m^{-3})	1657 \pm 170	—
ρ_{LP^*} , late Pleistocene bulk density (kg m^{-3})	—	1914 \pm 200
dz/dx , topographic gradient	0.25 \pm 0.05	0.25 \pm 0.05
q_v , volumetric sediment flux rate ($\text{m}^3 \text{ m}^{-1} \text{ a}^{-1}$)	0.0022 \pm 0.0007	0.0012 \pm 0.0005
K , soil transport rate constant ($\text{m}^2 \text{ a}^{-1}$)	0.0088 \pm 0.003	0.0047 \pm 0.002

*KOT—Kawakawa/Oruanui tephra (27,097 \pm 957 cal. yr B.P.)

¹GSA Data Repository item 2009230, Figure DR1 (depth profiles of ^{137}Cs activity measured at the interfluvium and valley fill sample sites), is available online at www.geosociety.org/pubs/ft2009.htm, or on request from editing@geosociety.org or Documents Secretary, GSA, P.O. Box 9140, Boulder, CO 80301, USA.

Increased late Pleistocene–Holocene transport on the slopes of Charwell Basin is coincident with an inferred decrease in sediment flux for the adjacent unglaciated mountains of the Seaward Kaikoura Range (Fig. 1B). In the uplands, geologic and topographic characteristics (specifically, fractured bedrock and steep slopes) ensure that sediment flux via landslides always exceeds that associated with bioturbation-driven soil transport. The reverse is true for the gentle, loess-mantled slopes of our study site. These opposing patterns of transport only reflect relative changes within each domain; in absolute terms, hillslope erosion rates for the upland catchment likely exceed those for the gentle Charwell Basin slopes at all times. Thus, catchments of the Seaward Kaikoura Range dominate the regional sediment budget.

We conclude that geologic and topographic factors have a first-order (and often overlooked) role in modulating how climate and vegetation change influence sediment transport and landscape evolution. Recent computer models have integrated ecological dynamics to predict patterns of channel network development, and these simulations require data of the kind presented here for calibration (e.g., Yoo et al., 2005). The colluvial infilling and phytolith records described here show that the transition to forested Holocene conditions led to a significant increase in the flux of soil on low-gradient, transport-limited slopes. Recognizing climate-driven, vegetation-mediated changes in sediment flux will improve our ability to predict the interplay between ecosystem shifts and landscape evolution, as well as constrain processes that control nutrient cycling and soil organic carbon storage.

ACKNOWLEDGMENTS

This study was part of the doctorate research of M.W. Hughes and was partially supported by National Science Foundation grant EAR-0309975 to Roering. Owners in Charwell Basin graciously provided access. We thank F. Shanhun and M. Smith for field assistance, and W. Bull, K. Yoo, J. Kaste, P. Molnar, and R. Westaway for thoughtful reviews.

REFERENCES CITED

Alloway, B.V., and 55 others, 2007, Towards a climate event stratigraphy for New Zealand over the past 30,000 years (NZ-INTIMATE project): *Journal of Quaternary Science*, v. 22, p. 9–35, doi: 10.1002/jqs.1079.

Bull, W.B., 1991, *Geomorphic responses to climate change*: New York, Oxford University Press, 326 p.

Denny, C.S., and Goodlett, J.C., 1956, Microrelief resulting from fallen trees: U.S. Geological Survey Professional Paper 288, p. 59–68.

Dietrich, W.E., and Perron, J.T., 2006, The search for a topographic signature of life: *Nature*, v. 439, p. 411–418, doi: 10.1038/nature04452.

Gabet, E.J., Reichman, O.J., and Seabloom, E.W., 2003, The effects of bioturbation on soil processes and sediment transport: *Annual Review of Earth and Planetary Sciences*, v. 31, p. 249–273, doi: 10.1146/annurev.earth.31.100901.141314.

Goossens, D., 1988, The effect of surface curvature on the deposition of loess: A physical model: *Catena*, v. 15, p. 179–194, doi: 10.1016/0341-8162(88)90027-6.

Istanbulluoglu, E., and Bras, R.L., 2005, Vegetation-modulated landscape evolution: Effects of vegetation on landscape processes, drainage density, and topography: *Journal of Geophysical Research (Earth Surface)*, v. 110, F02012, doi: 10.1029/2004JF000249.

Johnson, D.L., 1990, Biomantle evolution and the redistribution of Earth materials and artifacts: *Soil Science*, v. 149, p. 84–102, doi: 10.1097/00010694-199002000-00004.

Kaste, J.M., Heimsath, A.M., and Bostick, B.C., 2007, Short-term soil mixing quantified with fallout radionuclides: *Geology*, v. 35, p. 243–246, doi: 10.1130/G23355A.1.

Kirkby, M.J., 1971, Hillslope process-response models based on the continuity equation: *Institute of British Geographers Special Publication 3*, p. 15–30.

Lowe, D.J., Phil, A., Shane, A.R., Alloway, B.V., and Newnham, R.M., 2008, Fingerprints and age models for widespread New Zealand tephra marker beds erupted since 30,000 years ago: A framework for NZ-INTIMATE: *Quaternary Science Reviews*, v. 27, p. 95–126, doi: 10.1016/j.quascirev.2007.01.013.

McFadden, L.D., and McAuliffe, J., 1997, Lithologically influenced geomorphic responses to Holocene climatic changes in the Southern Colorado Plateau, Arizona: A soil-geomorphic and ecologic perspective: *Geomorphology*, v. 19, p. 303–332, doi: 10.1016/S0169-555X(97)00017-2.

McGlone, M.S., and Basher, L.R., 1995, The deforestation of the upper Awatere catchment, Inland Kaikoura Range, Marlborough, South Island, New Zealand: *New Zealand Journal of Ecology*, v. 19, p. 53–66.

Molnar, P., 2004, Late Cenozoic increase in accumulation rates of terrestrial sediment: How might climate change have affected erosion rates?: *Annual Review of Earth and Planetary Sciences*, v. 32, p. 67–89, doi: 10.1146/annurev.earth.32.091003.143456.

Norton, D.A., 1989, Tree windthrow and forest soil turnover: *Canadian Journal of Forest Research*, v. 19, p. 386–389, doi: 10.1139/x89-059.

Pillans, B.J., 1994, Direct marine-terrestrial correlations, Wanganui Basin, New Zealand: The last 1 million years: *Quaternary Science Reviews*, v. 13, p. 189–200, doi: 10.1016/0277-3791(94)90024-8.

Reneau, S.L., Dietrich, W.E., Dorn, R.I., Berger, C.R., and Rubin, M., 1986, Geomorphic and paleoclimatic implications of latest Pleistocene radiocarbon dates from colluvium-mantled hollows, California: *Geology*, v. 14, p. 655–658, doi: 10.1130/0091-7613(1986)14<655:GAPIOL>2.0.CO;2.

Roering, J.J., Almond, P., McKean, J., and Tonkin, P., 2002, Soil transport driven by biological processes over millennial timescales: *Geology*, v. 30, p. 1115–1118, doi: 10.1130/0091-7613(2002)030<1115:STDBBP>2.0.CO;2.

Roering, J.J., Almond, P., Tonkin, P., and McKean, J., 2004, Constraining climatic controls on hillslope dynamics using a coupled model for the transport of soil and tracers: Application to loess-mantled hillslopes, Charwell River, South Island, New Zealand: *Journal of Geophysical Research (Earth Surface)*, v. 109, F01010, doi: 10.1029/2003JF000034.

Schaetzl, R.J., Burns, S.F., Small, T.W., and Johnson, D.L., 1990, Tree uprooting: Review of types and patterns of soil disturbance: *Physical Geography*, v. 11, p. 277–291.

Shuster, D.L., Ehlers, T.A., Rusmore, M.E., and Farley, K.A., 2005, Rapid glacial erosion at 1.8 Ma revealed by ⁴He/³He thermochronometry: *Science*, v. 310, p. 1668–1670, doi: 10.1126/science.1118519.

Tonkin, P.J., and Almond, P.C., 1998, Using loess soil stratigraphy to reconstruct the late Quaternary history of piedmonts adjacent to large strike slip faults, South Island, New Zealand: *Geological Society of New Zealand Miscellaneous Publication 101A*, p. 227.

Wallace, L.M., Beavan, J., McCaffrey, R., Berryman, K., and Denys, P., 2007, Balancing the plate motion budget in the South Island, New Zealand using GPS, geological and seismological data: *Geophysical Journal International*, v. 168, p. 332–352.

Wardle, P., 1991, *Vegetation of New Zealand*: Cambridge, UK, Cambridge University Press, 672 p.

Yoo, K., Amundson, R., Heimsath, A.M., and Dietrich, W.E., 2005, Process-based model linking pocket gopher (*Thomomys bottae*) activity to sediment transport and soil thickness: *Geology*, v. 33, p. 917–920, doi: 10.1130/G21831.1.

Zhang, P., Molnar, P., and Downs, W.R., 2001, Increased sedimentation rates and grain sizes 2–4 Myr ago due to the influence of climate change on erosion rates: *Nature*, v. 410, p. 891–897.

Manuscript received 20 February 2009

Revised manuscript received 15 April 2009

Manuscript accepted 21 May 2009

Printed in USA